INCLUSION DEFORMATION:
I. THE MECHANISM OF FRACTURE AND DEFORMATION IN MnS

by H. C. Chao, L. Thomassen, and L. H. Van Vlack*

ABSTRACT:

Manganese sulfide was purified and crystallized from a melt, obtaining the stable (NaCl-type) structure. Single crystals were used to determine the glide and fracture systems. The primary glide system is [[110]] ((110)). Secondary slip occurs on the ((111)) planes. There was no evidence of ((100)) deformation. Although ((100)) cleavage is predominant, ((110)) cleavage is observed and becomes the primary fracture plane when the MnS is loaded by surface indentation. The ((110)) fracture originates through (a) the interaction of dislocation movements on the $((110))_{45^\circ}$ planes, and (b) the interaction of ((111)) slip planes at the (110) surface.

---

* H. C. Chao is a graduate student, and L. Thomassen and L. H. Van Vlack are professors, Department of Chemical and Metallurgical Engineering, The University of Michigan, Ann Arbor, Michigan.

INTRODUCTION

Whenever sulfide inclusions are present within steels, it is desirable to have the sulfur present as alabandite, or MnS. Manganous sulfide has a higher melting temperature than FeS (1620°C vs 1200°C) and therefore does not contribute to hot-shortness of the steel during shaping operations. Also, in free-machining steels where sulfur is intentionally added to steel, the sulfide must have the alabandite structure to be effective.

A steel normally has its strength, ductility, and impact resistance lowered when it contains sulfide inclusions. Therefore, a solid sulfide phase is usually considered to be a brittle, non-ductile material. In reality, manganese sulfide can be deformed prior to fracture. This deformation is most obvious in hot-rolled steel where the inclusions have developed an elongated shape (Fig. 1). Also, it has been suggested (but never fully proven) that the improved machinability of resulfurized steel does not depend entirely upon the weakening of the steel by the inclusions for easier chip formation, but also upon a lubricating action of the sulfide phase at the tool surface.[1,2] Direct evidence of the plastic deformation of MnS has been observed recently at room temperatures in two cases. The first was in massive MnS,[3] and the second was within sulfide inclusions in steel.[4]

This paper presents the results of an investigation to determine the dependence of fracture and deformation in MnS upon crystollographic factors.

PREVIOUS WORK

Structure and Composition. The stable form of MnS has the NaCl-structure. In addition, Kröger[5] found that MnS will crystallize with both the ZnO and ZnS-structures from selected aqueous solutions, and Rooksby and Tombs[6] report a rhombehedral structure at liquid air temperatures. This present investigation is limited to the NaCl-type structure.

The stoichiometry of MnS has not received detailed attention. However, the commonly reported one-to-one ratio of manganese-to-sulfur ions is apparently valid because related work[7] by the authors showed 36.8±0.2 percent. The balanced composition of MnS is in contrast to the cation deficient FeS structure of pyrrhotite where the sulfur content varies from 37 to 42 percent[8] (vs. 36.5 percent in stoichiometric FeS).

Anion solid solution in MnS is limited. Concurrent work[7] revealed a maximum of 1.7 weight percent MnO in MnS which corresponds to a replacement of approximately 2 percent of the sulfur ions by oxygen ions. Cation solid solution is more extensive. Kröger[5] reports zinc and cadmium substitution for manganese. Of more importance to nonmetallic inclusion work is the fact that there is rather extensive replacement of manganese by iron.

Wentrup[9] reports a maximum of 75 percent replacement near 1200°C. Current work[10] shows a maximum of 72 percent at 1181°C.

Deformation and Fracture. Except for a brief note,[4] no previous work has been reported on the deformation or fracture of MnS. However, since the structure of MnS is the same as that of NaCl, LiF and MgO, attention should be given to their behavior under mechanical stressing. Gilman[11] gives a complete review and indicates that, except for PbS and PbTe which are highly polarizable, all rock salt-type crystals have a [110] glide direction and a (110) glide plane for primary deformation. His review included MgO, LiF, NaF, NaCl, NaBr, NaI, KCl, KBr, KI, RbCl, NH_3l, AgCl and AgBr. In addition, secondary glide systems were reported as [[110]] ((100)) on most of the above halides. Buerger[12] reported [[110]] ((111)) glide in the sodium halides. It is significant that all reported glide directions are the [[110]] directions, even in PbS and PbTe. Also of interest is the fact that the [[110]] ((100)) glide system has not been reported for periclase (MgO).

Keh[13] used surface indentations to study the deformation of single crystals of periclase. After indentation, etch rosettes appeared in the (100) surfaces which permitted the interpretation of dislocation movement. Only the [[110]] ((110)) glide system was identified.

The hardness of MnS decreases as the temperature is increased.[10] This indicates that slip occurs more readily with increased temperatures, much as expected.

Fracture in the NaCl-type crystals is characterized by ((100)) cleavage. Gilman[11] reports secondary cleavage on the ((110)) planes as does Keh[13] who concluded that they were the result of interactions of dislocations on the $((110))_{45^\circ}$ planes, (i.e., ((110)) planes which are inclined at 45° to the external (100) indentation surface). The relative energies required for the formation of the ((100)) and the ((110)) surfaces by cleavage has been calculated for alkali halides by Van Zeggeren and Benson[14] who indicate that the energy for the latter planes should be from 2 to 5 times the energy for the ((100)) planes.

EXPERIMENTAL PROCEDURE

Manganese sulfide was purified and prepared in both the single crystal and polycrystalline forms. Pyramid indentation was used to analyze the deformation systems.

MnS purification. Although several procedures were used to prepare MnS for subsequent melting and crystal growth (Appendix A), only the procedure yeilding the purest MnS will be described here. It utilized a sulfur deoxidation of reagent grade manganese sulfate as shown in Fig. 2. In essence, sulfur was vaporized at 410°C and one atmosphere pressure before coming in contact with $MnSO_4$ powder at 900°C. The relationship,

$$MnSO_4 + S_2 \longrightarrow MnS + 2SO_2 \ ,$$

appears to be appropriate. When the reaction was completed, it

gave an analysis of 36.8±0.2 percent sulfur. The metal ion content is shown in Table 1. Neither x-ray diffraction nor optical examination revealed other phases; however, it became apparent that in powder form the surface would oxidize with time. Therefore, the purified MnS powder was melted and solidified for later use. The lattice constant for the purified MnS was 5.225A, as compared to the value of 5.224A reported by ASTM.[15]

A second and third type of manganese sulfide sample were used in this study. (2) Manganese sulfide with about one percent calcium is listed in Table 1. Microscopic and diffraction data indicated that the calcium ion entered the alabandite (MnS) as a solid solution; a = 5.232A. However, there was some indirect evidence of precipitation at elevated temperatures. (3) The third type was manganese sulfide which contained minor amounts of MnO as a grain boundary precipitate. This meant that the MnO slightly exceeded 1.7 percent.[7]

Sample preparation. All of the MnS was briefly melted and solidified in a graphite crucible before analyses were made. In a few cases this product was used directly as polycrystalline MnS. However, most of the MnS in this study was used as large crystals for single crystal examination.

Three procedures were utilized for single crystal preparation. These include: (1) the vapor depositions of MnS by iodide transport, (2) a Bridgman cell technique, and (3) a zone refining procedure. The latter proved to be most satisfactory and will be described briefly. (The others are described in Appendix B.) About 60 gms

of the previously melted MnS were crushed to about 3 mm and remelted under a purified argon and/or nitrogen atmosphere in a graphite boat within a horizontal moving coil induction furnace. After two or three initial passes, a final pass was made at the rate of about 1 inch per hour in which time a coarsely crystalline (up to 1 cm) grain size developed. Fracturing revealed cleavage planes which were used for orientation checks and as guides for further cutting.

Fracture and Deformation tests. A diamond hardness indentor was used for fracture and deformation. Cleavage was used to locate the (100) surfaces. However, these were generally polished and etched prior to indentation. Other crystal planes were ground to the correct orientation before polishing, etching and indenting.

Slip lines were directly observable after indentation on the previously prepared surface. The dislocation lines were revealed by etching with three percent of equal parts of concentrated H_2SO_4, concentrated H_3PO_4, and a saturated solution of oxalic acid.

RESULTS AND DISCUSSION

Fracture. Both grain boundary and cleavage fracture were observed within the samples. The grain boundary fracture was a direct consequence of the precipitation of small quantities of nearly submicroscopic particles of MnO at the boundary. It can not be concluded from this investigation that MnO is inherently

more brittle than MnS because the fracture may be controlled by the phase boundary. However, the presence of the MnO changes the fracture characterization markedly so that individual MnS grains are separable. In the absence of observable oxide precipitation, cleavage fracture predominates in polycrystalline MnS.

The ((100)) planes are the most prominent cleavage surfaces when grains are crushed. Additional secondary cleavage is developed on the ((110)) planes, often observable as oblique offsets to the ((100)) cleavage (Fig. 3). The preceding observations are directly correlatable to other compounds with the NaCl structure.[11]

Indentation tests favor fracture along the ((110)) planes (Fig. 4 a and b). Although deformation has not been discussed as yet, it may be noted here that the ((110)) planes are the principal slip planes, and movements along the several $((110))_{45^\circ}$ planes would induce tensile stresses at the surface of the sample normal to the $((110))_{90^\circ}$ planes. Thus the fracture in MnS may be considered to be analogous to that in periclase (MgO) as determined by Keh.[13] The absence of ((100)) cleavage should be expected in samples deformed by indentation because the movement along the several $((110))_{45^\circ}$ planes is parallel to the $((100))_{90^\circ}$ planes, and the location of tensile stresses from $((110))_{90^\circ}$ displacement are in the compressive zone below the indentor.

The role of temperature upon cleavage is complicated by the simultaneous change in plastic deformation. Because plastic

deformation does occur more readily at higher temperatures, the relative amount of fracture is reduced.

Deformation. Results and interpretation of deformation of MnS was obtained by three procedures. The first of these included measurements of the broadening of x-ray diffraction lines, followed by annealing at increasingly higher temperatures. The second was through the study of etch pits of dislocation lines that terminated on the crystal surfaces, and the third involved the examination of slip lines on the crystal surfaces.

Diffraction lines of powdered MnS are too broad to permit accurate lattice parameter measurements, thus indicating plastic distortion of the crystal structure. The line broadening must be attributed to deformation rather than fine grain size because subsequent heating permitted annealing and gave a measurable sharpening of the diffraction lines as shown in Fig. 5.

Dislocations were revealed by etch pit rosettes as shown in Fig. 6 and 7. The patterns of dislocation are identical to those discussed by Keh[13] for periclase (MgO), and may be interpreted as follows. The indentor displaces MnS along the ((110)) planes in the [[$\bar{1}$10]] directions, and in effect provides a dislocation "loop" which swings under the indentation emerging on the other side.

Both edge and screw dislocations are observed, with the edge dislocation emerging perpendicular to the (100) etch surface and the screw dislocations emerging at 45° to the (100) surfaces. In MnS the edge dislocations are more readily etched than the screw dislocations. This agrees with the behavior in MgO.[16]

If planes other than ((100)) are used as an indenting surface, the dislocation etch pits are less obvious, but present (Fig. 8). This difference is a consequence of the plane of etching rather than the deformation mechanism or the dislocation alignment, because the difference may be revealed on the same samples as those which possess good etching characteristics on the (100) planes. It may be concluded that the ((110)) planes of MnS are relatively stable in the etchant solution which was used. Not only are the dislocations poorly revealed on a (110) surface, but also, the ((110)) facets are those remaining in the dislocation pits on a (100) surface (Fig. 9).

At higher temperatures, the etch pit rosettes are more diffuse but involve more dislocations (Fig. 10). In effect, plastic deformation is nucleated more generally.

Slip traces from deformation are revealed without etching, but with oblique illumination if the crystal surface is polished before indentation (Fig. 11). There has been an upward displacement of the surface along $((110))_{45^\circ}$ planes. However, it may be shown that slip along any particular side of the indentor is not a simple displacement along parallel $(110)_{45^\circ}$ planes. Rather, slip occurs along two sets of $(110)_{45^\circ}$ planes as indicated in Fig. 12 and interpreted from Fig. 13. In the latter figure, the surface used for indentation was inclined a few degrees from the (001) plane through a rotation around the [100] axis. As such, the surface traces of the two sets of planes in Fig. 13(b) are skewed in opposite

directions so that they are not parallel (Fig. 13a). These results also exclude the possibility of secondary slip on the ((100)) planes because this type of crystal inclination would not alter the traces at the surface.

Secondary slip was observed on ((111)) planes as illustrated in Fig. 14. These slip traces can not arise from ((110)) planes because they would require movement in a [100] direction, a direction which has extremely high ion repulsion. The secondary slip on the ((111)) planes is often associated with the $((110))_{90°}$ fracture (Fig. 14b). The sequence of events appears to be: (1) fracture along the $(110)_{90°}$, (2) progression of slip deformation on closely associated (111) planes, and then (3) fracture on the complementary $(110)_{90°}$ plane in the vicinity of the (111) slip. As such, the latter $(110)_{90°}$ fracture would arise from interaction of dislocation movements in the ((111)) planes, much as the initial $(110)_{90°}$ fracture arose from dislocation movements in the $((110))_{45°}$ planes.[13] Neither the reason for the periodic location of the ((111)) slip lines along the $(110)_{90°}$ crack nor direction of the slip along these planes is known; however, it may be concluded that their explanation, as well as that of the (111) slip proper, must take into account the (110) surface which has been exposed.

CONCLUSIONS

(1) The deformation and fracture of manganese sulfide in its alabandite form may be compared directly with other NaCl-type compounds.

(2) The primary glide system in MnS is [[110]] ((110)) and is easily revealed as slip traces or as dislocation etch pits.

(3) A secondary glide system involving ((111)) planes developed subsequent to $((110))_{90^\circ}$ fracturing. There was nc evidence of secondary ((100)) glide planes.

(4) Grain boundary fracture occurs in MnS when a minor amount of MnO is present.

(5) Primary fracture occurs as ((100)) cleavage. However, ((110)) cleavage steps may be observed on the ((100)) surfaces.

(6) The $((110))_{90^\circ}$ cleavage becomes the primary fracture system during surface loading. Such fracture develops by the interaction of $((110))_{45^\circ}$ slip and the (001) surface; in addition, a minor amount of $((110))_{90^\circ}$ fracture can occur through the interaction of ((111)) slip and the (110) surface.

ACKNOWLEDGEMENTS

The authors wish to acknowledge the support of the Edgar C. Bain Research Laboratory of U. S. Steel. Specific thanks should be given to Drs. R. Rickett and A. S. Keh for their critical discussions and suggestions.

REFERENCES

1. F. W. Boulger, Machining -- Theory and Practice, ASM, Metals Park, Ohio, (1950) 77.
2. J. D. Armour, Machining -- Theory and Practice, ASM, Metals Park, Ohio, (1950) 136.
3. L. H. Van Vlack, O. K. Riegger, R. J. Warrick, J. M. Dahl, Sulfide Inclusions in Steel, Trans. AIME, 221 (1961) 227.
4. L. Wood and L. H. Van Vlack, Fracture and Deformation of Sulfide Inclusions in Steel, Technical Note. Submitted for publication.
5. F. A. Kröger, Solid Solutions in the Ternary System ZnS-CdS-MnS, Zeit. f. Krist., 102A (1939) 132.
6. H. P. Rooksby and N. C. Tombs, Structure of Monoxides of some Transition Elements at Low Temperatures, Nature, 165 (1950) 442.
7. H. C. Chao, Y. E. Smith, and L. H. Van Vlack, The MnO-MnS Phase Diagram, Technical Note. To be submitted for publication.
8. J. Chipman, Fe-S Iron-Sulfur, Metals Handbook, ASM, Metals Park, Ohio, (1948) 1215.
9. H. Wentrup, Die Bildung von Einschlüssen im Stahl, Tech. Mitt. Krupp, 5 (1937) 139.
10. H. C. Chao, L. H. Van Vlack and L. Thomassen, Inclusion Deformation II. Hardness of FeS-MnS Microstructures. To be submitted for publication.

11. J. J. Gilman, Mechanical Behavior of Ionic Crystals, Progress in Ceramic Science, J. E. Burke, Pergamon Press, New York, (1961) 146.

12. M. J. Buerger, Translation-Gliding in Crystals, Amer. Mineralogist, 15 (1930) 45.

13. A. S. Keh, Dislocations in Indented Magnesium Oxide Crystals, Journ. App. Phys., 31 (1960) 1538.

14. F. Van Zeggener and G. C. Benson, Calculation of the Surface Energies of Alkali Halide Crystals, Journ. Chem. Phys., 26 (1957) 1077.

15. Swanson, et al., N.B.S., Circular 539, IV, (1955) 11.

16. R. M. Fulrath, personal communication.

TABLE I

The Impurity Level of Three Types of MnS

Elements	Samples 1 & 3 (pure) %	Sample 2 (with 1% Ca) %
Ca	0.01	1.0
Mg	0.001	0.1
Fe	0.003	0.1
Ti	0.003	0.01
Cr	0.0003	0.005
Ni	0.001	0.002
Al	0.02	0.02
Cu	0.0002	0.0005

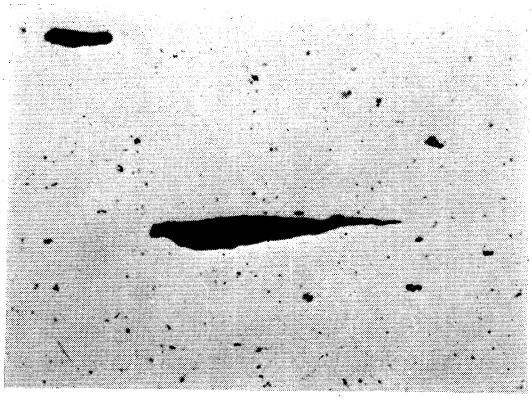

Fig. 1. Sulfide inclusions deformed by hot-rolling. Example: desulfurized steel. X500.

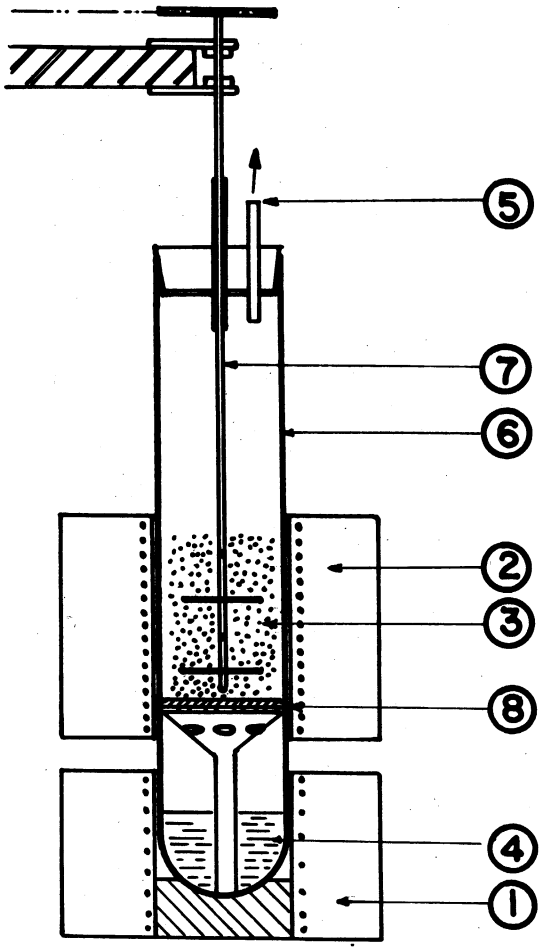

Fig. 2. MnS purification. Reagent grade $MnSO_4$ was deoxidized with sulfur vapor.
(1) Lower furnace, 410°C.
(2) Upper furnace, 900°C.
(3) $MnSO_4$ charge.
(4) Liquid sulfur.
(5) SO_2 exhaust.
(6) Reaction tube.
(7) Stirrer.
(8) Support of graphite felt and a porcelain filter to hold the change.

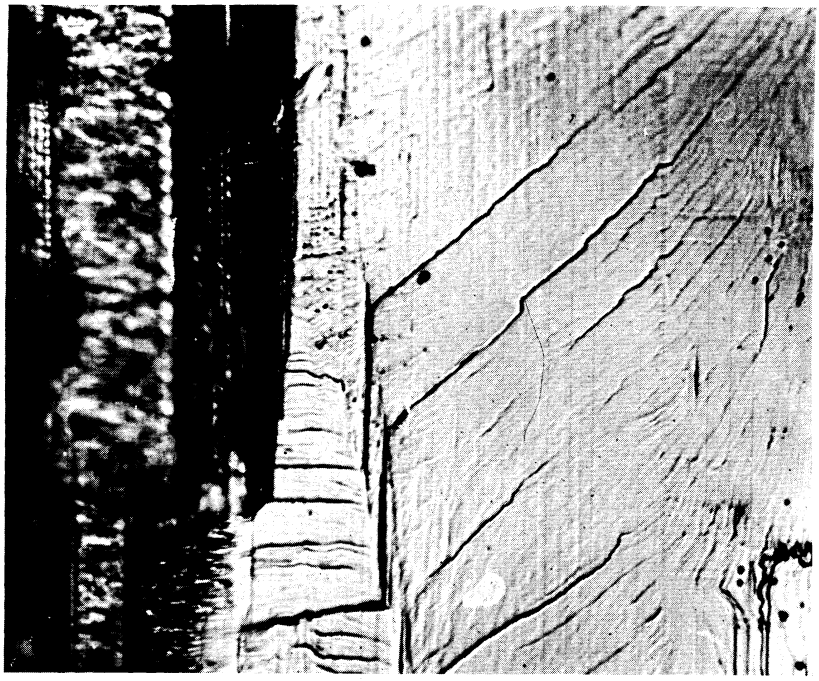

Fig. 3. MnS cleavage surface (001). Cracks also form at 45° to the [100] direction. X500.

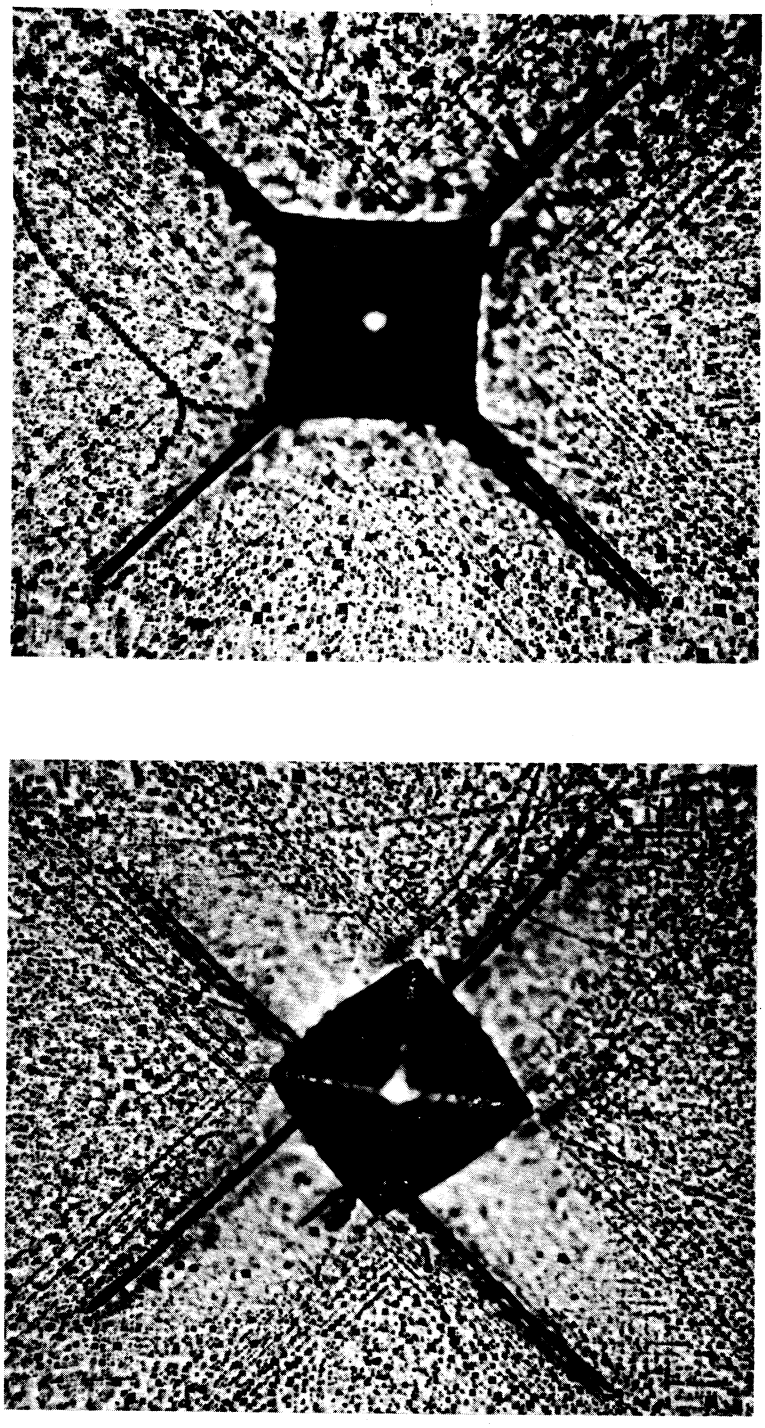

Fig. 4. Fracture in MnS from indentation. (a) Cracks are formed along (110) planes normal to the (001) surface. (b) The indentor is rotated 45°. X500.

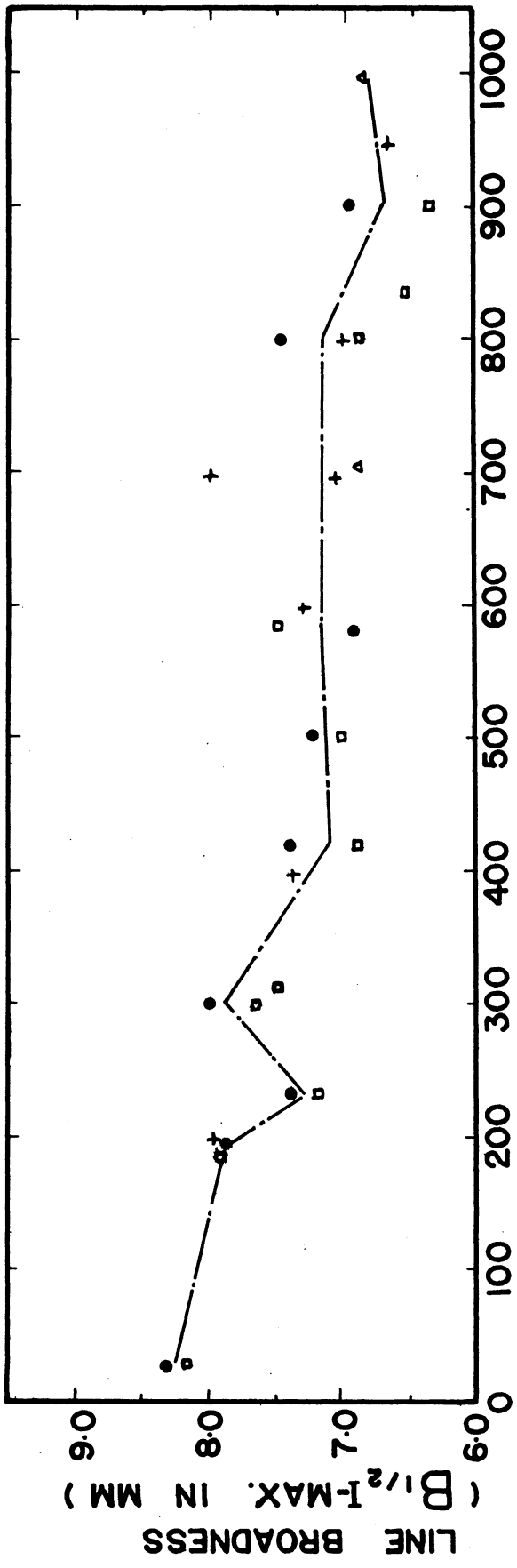

Fig. 5. Line broadness vs. annealing temperature.

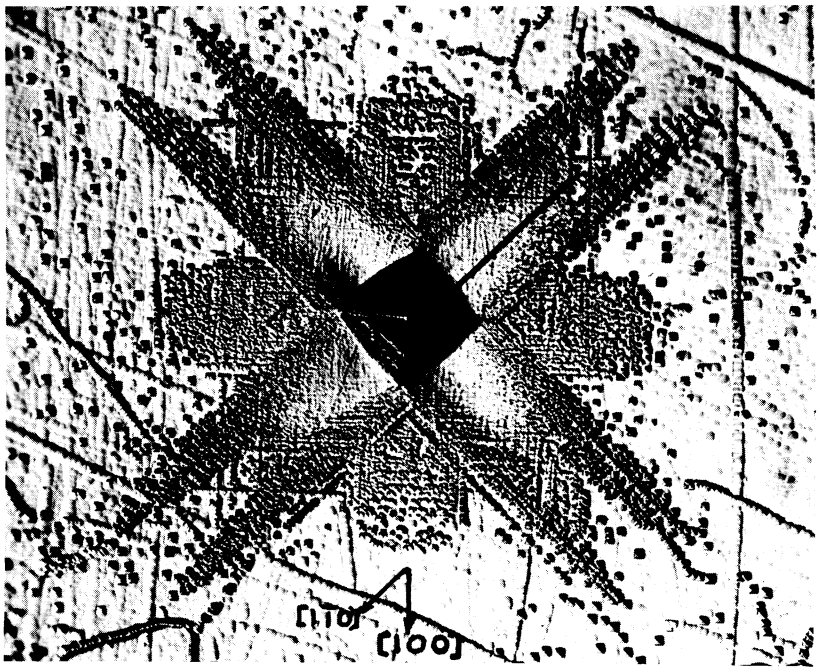

(a)

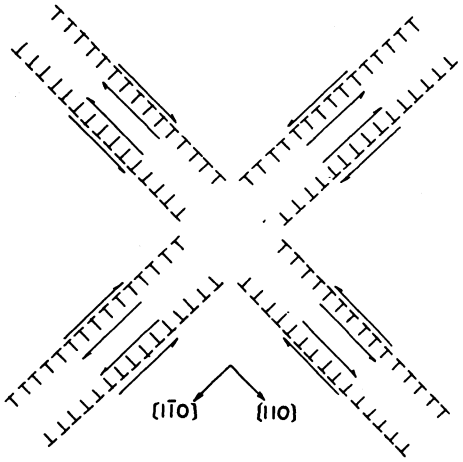

(b)

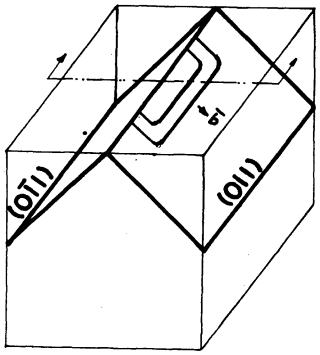

(c)

Fig. 6. Dislocation rosette. Example: (001) surface. (a) Etched after indentation. X250. (b) Edge dislocation development on the $((110))_{90°}$ planes. See Fig. 7 for the dislocations with the $((110))_{45°}$ planes. (c) $((110))_{90°}$ planes and dislocation lines. Buerger's vector is 110 .

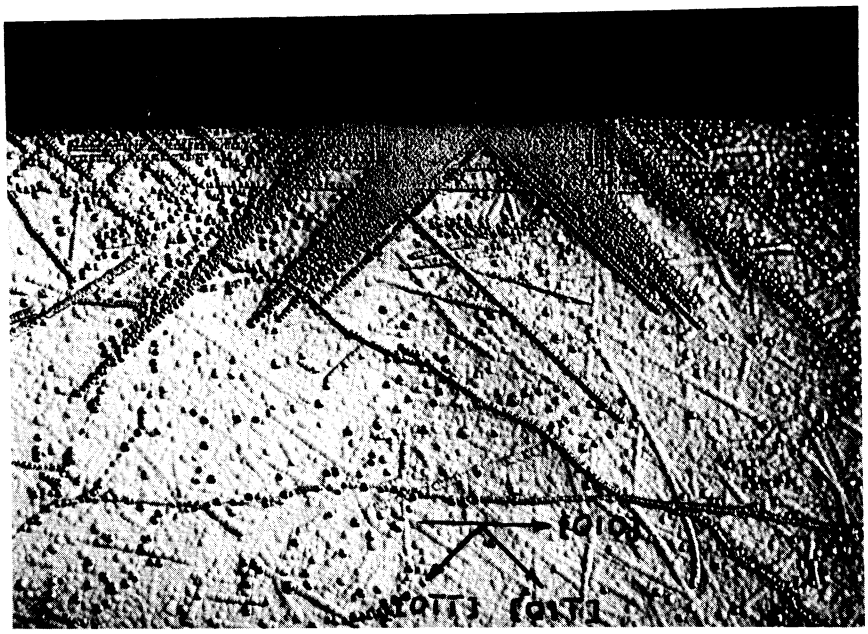

(a)

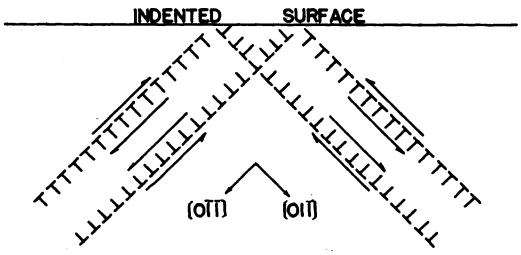

(b)

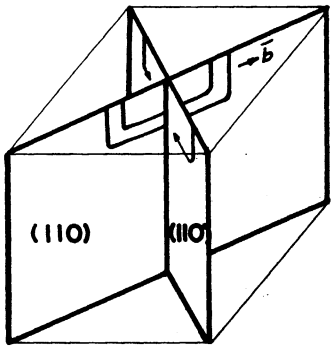

(c)

Fig. 7. Dislocation rosette (vertical cross-section). (a) The MnS crystal of Fig. 6 was ground to below the indentation, then cleaved on the (100) plane, polished and etched. X250. (b) Edge dislocation development on the $((110))_{45°}$ planes. These appear as screw dislocations in Fig. 6. (c) $((110))_{45°}$ planes and dislocation lines. Buerger's vector is [110].

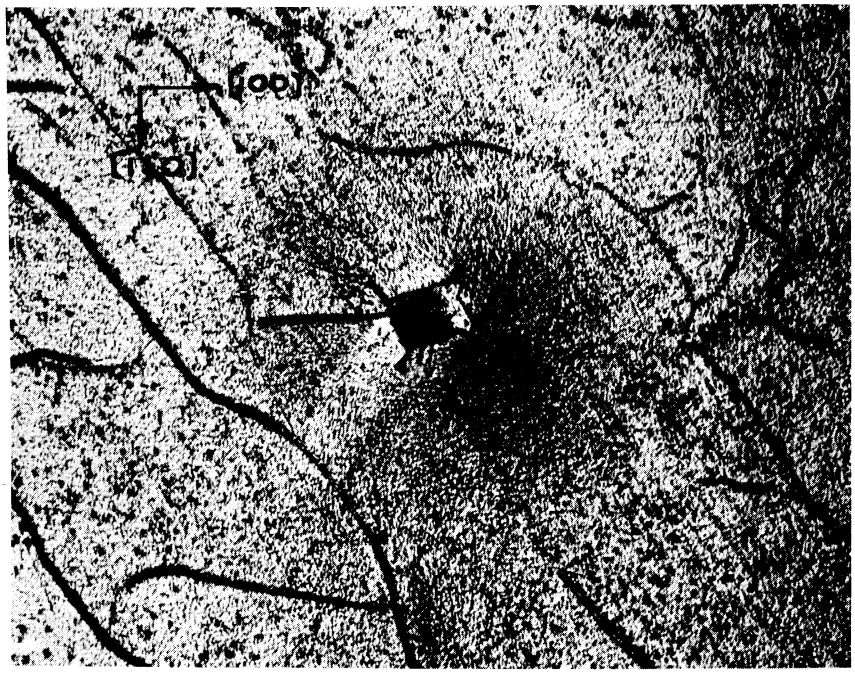

Fig. 8. Dislocation rosette on a (110) surface. The more rapid etching of the (110) surface prevented good rosette development. X200.

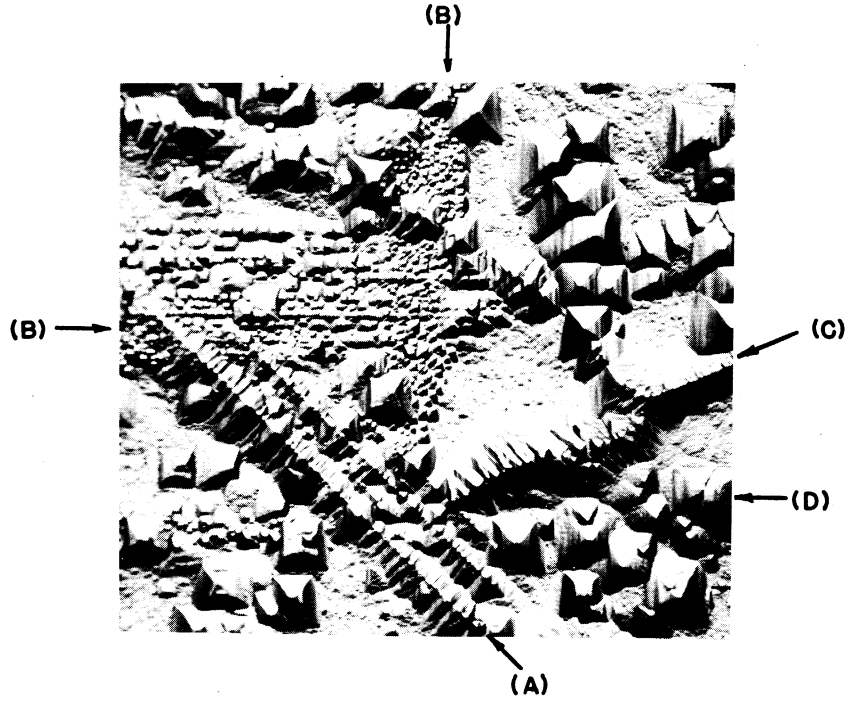

Fig. 9. Dislocation etch pits. (a) Edge dislocations from $(110)_{90°}$ planes. (b) Screw dislocations from $(110)_{45°}$ planes. (c) Small angle boundary. (d) Random dislocations. In each case the ((110)) surfaces are developed. X500.

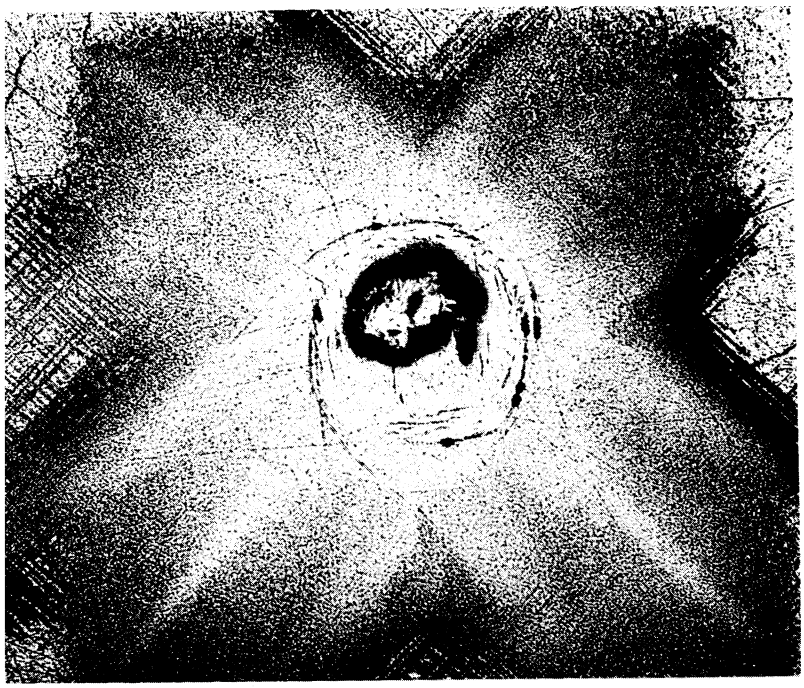

Fig. 10. Dislocation rosette from 700°C indentation. No ((110)) cleavage cracks were formed above 300°C. X100. (The indentor was spherical in this case; however, cracks were also absent with pyramid indentations.)

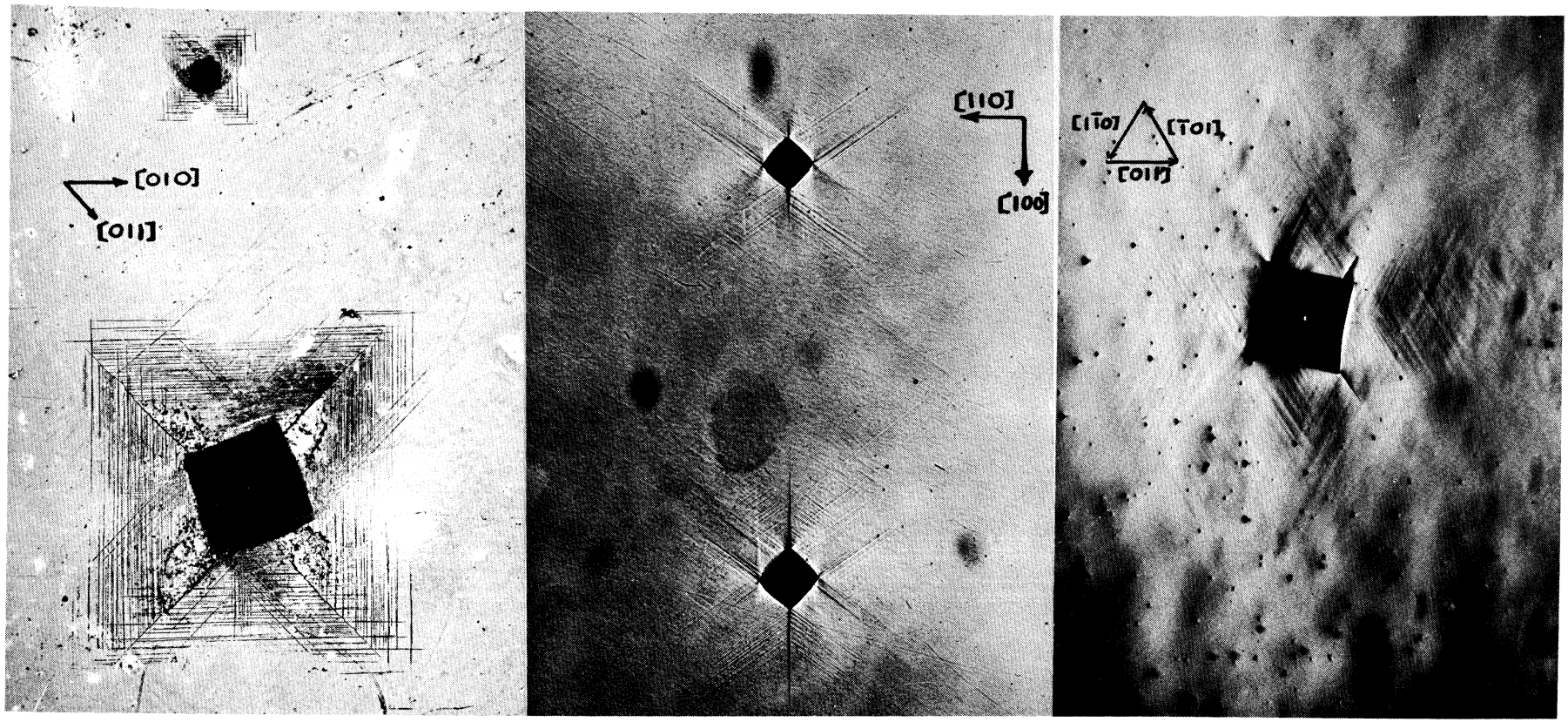

(a) (b) (c)

Fig. 11. Slip traces from ((110)) deformation. (a) (100) plane. The traces were revealed by previous surface oxidation. Two loads were used. (b) (110) plane. (c) (111) plane. In (b) and (c) the traces were revealed by oblique illumination.

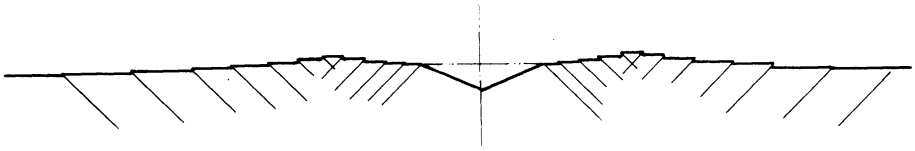

Fig. 12. Multiple $((110))_{45°}$ slip adjacent to the indentor. See Fig. 13.

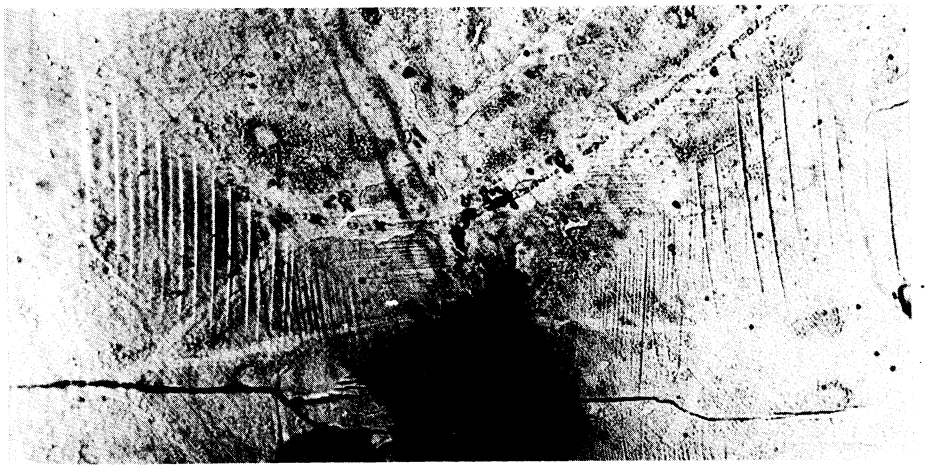

(a)

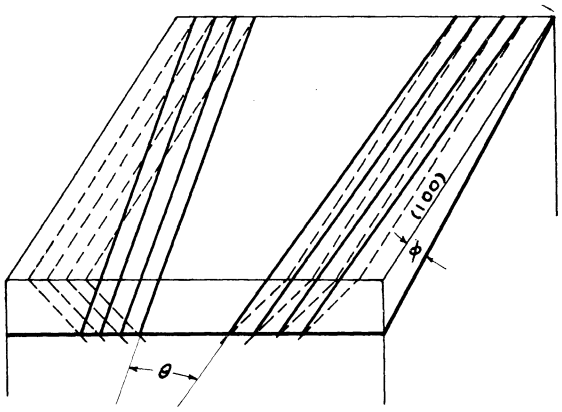

(b)

Fig. 13. Multiple slip planes. (a) Indentation surface tilted 5.5° from (100). X100. (b) Sketch of disaligned slip traces. The angle $\theta \cong 2\phi$ for small tilt angles, ϕ.

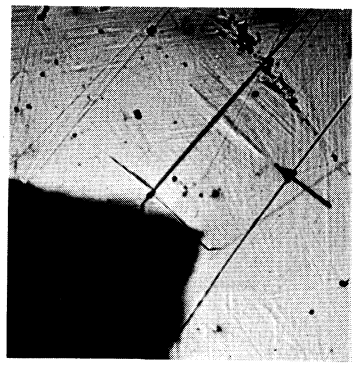

(a)

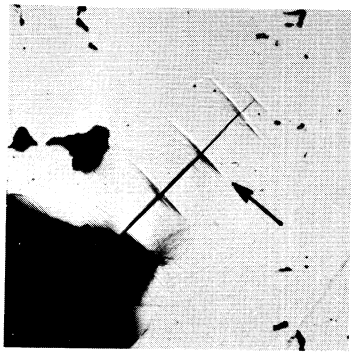

(b)

Fig. 14. (a) ((111)) deformation (arrow). Also see the large indentation of Fig. 11(a). These 45° slip lines can not arise from ((110)) slip. They lead to (110) fracture. Examples: (a) (Mn,Fe)S with 75/25 Mn/Fe ratio; (b) (Mn,Fe)S with 50/50 Mn/Fe ratio. X100. Oblique illumination.

APPENDIX A*

ALTERNATE METHODS OF PREPARING MnS

Alternate methods of preparing MnS are summarized in Table A-1. In each case trace amounts of MnO were always present in the final product. In addition, sulfur condensation problems arose in the exit end of the equipment. The previously described sulfur deoxidation procedure is preferred.

---

* This appendix, which is included in the report for record, will not be incorporated into the published version.

TABLE A-1. Gas Treatment of MnS (850-900°C)

	Starting Material	
	Commercial MnS	"Reagent" $MnSO_4$
Dry Argon + CS_2	X	
Dry Nitrogen + CS_2	X	X
Dry Nitrogen + H_2		X
Dry Nitrogen + H_2 + H_2S		X

APPENDIX B*

ALTERNATE METHODS OF SINGLE CRYSTAL GROWTH

Two alternate methods of single crystal preparation were utilized with incomplete success. These included (1) an iodide vapor transport procedure and (2) a Bridgeman cell procedure.

The iodide vapor transport procedure utilized purified MnS powder which was sealed in an evacuated vycor tube with a side-arm containing AuI_3. The latter was thermally dissociated and the I_2 collected in the main tube before removing the side-arm. The tube was then exposed to a thermal gradient of 950°C at the MnS powder end, and 550°C at the other end. New MnS crystals grew at mid-gradient. Of prime interest was the fact that the MnS crystals formed plates in which the main surface was (111). However, only a few crystals could be made to exceed 1 mm. in their greatest dimension.

The Bridgeman cell was a graphite mold with a cavity of 1 cm. diameter and 6.6 cm. length plus a constricted 2 mm. neck at the base for seeding. A dried nitrogen atmosphere and a zone refining procedure were used for heating with the induction coil moving vertically past the constriction. Successful results were not obtained. The limitations of the procedure arose from extraneous vibrations and from the inability to know the temperature in the part of the MnS ingot which could not be seen. The range of temperature is narrow between MnS melting and MnS dissociation to manganese carbide and sulfur gas.

---

* This appendix, which is included in the report for the record, will not be incorporated into the published version.